JOURNAL OF BACTERIOLOGY, Oct. 2009, p. 6145–6156 Vol. 191, No. 19
0021-9193/09/$08.00+0 doi:10.1128/JB.00460-09

Hopanoids Play a Role in Membrane Integrity and pH Homeostasis in *Rhodopseudomonas palustris* TIE-1▽†

Paula V. Welander,[1] Ryan C. Hunter,[1] Lichun Zhang,[2] Alex L. Sessions,[2] Roger E. Summons,[3] and Dianne K. Newman[1,3,4]*

Department of Biology, Massachusetts Institute of Technology, 77 Massachusetts Avenue, 68-380, Cambridge, Massachusetts 02139[1]; Division of Geological and Planetary Sciences, California Institute of Technology, Pasadena, MC100-23, 1200 E. California Boulevard, Pasadena, California 91125[2]; Department of Earth, Atmospheric and Planetary Science, Massachusetts Institute of Technology, 77 Massachusetts Avenue, E25-633, Cambridge, Massachusetts 02139[3]; and Howard Hughes Medical Institute, 77 Massachusetts Avenue, 68-171, Cambridge, Massachusetts 02139[4]

Received 3 April 2009/Accepted 6 July 2009

Sedimentary hopanes are pentacyclic triterpenoids that serve as biomarker proxies for bacteria and certain bacterial metabolisms, such as oxygenic photosynthesis and aerobic methanotrophy. Their parent molecules, the bacteriohopanepolyols (BHPs), have been hypothesized to be the bacterial equivalent of sterols. However, the actual function of BHPs in bacterial cells is poorly understood. Here, we report the physiological study of a mutant in *Rhodopseudomonas palustris* TIE-1 that is unable to produce any hopanoids. The deletion of the gene encoding the squalene-hopene cyclase protein (Shc), which cyclizes squalene to the basic hopene structure, resulted in a strain that no longer produced any polycyclic triterpenoids. This strain was able to grow chemoheterotrophically, photoheterotrophically, and photoautotrophically, demonstrating that hopanoids are not required for growth under normal conditions. A severe growth defect, as well as significant morphological damage, was observed when cells were grown under acidic and alkaline conditions. Although minimal changes in *shc* transcript expression were observed under certain conditions of pH shock, the total amount of hopanoid production was unaffected; however, the abundance of methylated hopanoids significantly increased. This suggests that hopanoids may play an indirect role in pH homeostasis, with certain hopanoid derivatives being of particular importance.

Bacteriohopanepolyols (BHPs) are a class of pentacyclic triterpenoids, generally referred to as hopanoids, that are found in a variety of bacteria. Bacterial hopanoids have been hypothesized to be surrogates of eukaryotic sterols primarily because of similarities in their biosynthesis and structure (Fig. 1 A and B) (36). Sterols have been shown to play an important role in stabilizing eukaryotic cell membranes and regulating membrane fluidity, as well as providing resistance to ethanol and heat shock stress (20, 57, 61). Sterols are produced by all eukaryotes, and the membranes of animals, plants, and fungi have been shown to contain different types of sterols possibly with different physiological roles (20). Usually, these sterols vary in their patterns of A-ring and side chain alkylation and unsaturation (16, 20, 40). There are also a variety of sterol esters and steryl glycosides found in plants and yeast (41, 47). Regardless of which sterols are produced by eukaryotic cells, all eukaryotic organisms require these molecules to survive (40).

Hopanoids have been shown to localize to the cytoplasmic and outer membranes of certain bacteria (21, 24, 54), and in vitro experiments have shown that these molecules are efficient in condensing artificial membranes and enhancing the viscosity of liposomes (3, 43). As with eukaryotic sterols, there is also structural variation in hopanoids, where some are methylated at the C-2 or C-3 position and some are unsaturated, and the functionalization of the side chain can differ greatly (59). To date, no genetic, biochemical, physiological, or environmental studies have been done that explain the biological significance of these modifications. A few studies have proposed that hopanoids enhance membrane stability and decrease membrane permeability in some bacteria, including *Alicyclobacillus acidocaldarius* (43), *Zymomonas mobilis* (19), *Frankia* sp. (4), and *Streptomyces coelicolor* (44). However, these studies did not utilize a genetic approach or in vivo experiments to conclusively elucidate the role of hopanoids in membrane structure and stability. Thus, the extent to which they are sterol surrogates remains an open question.

While understanding the function of hopanoids is interesting from a purely cell biological perspective, there is an additional motivation provided by evolutionary biology. Geochemists and geobiologists frequently utilize these compounds as "molecular fossils" or biomarkers (8). In this context, biomarkers are organic compounds that are preserved in ancient sedimentary rocks and can be linked to specific organisms by analogy with their production in modern organisms (8, 9). The use of these molecular fossils has proven to be a powerful approach to study and reconstruct both ancient and modern microbial ecosystems (8). Sedimentary hopanes comprise one of the most abundant and ubiquitous types of extractable organic compounds in ancient rocks (8) and are unambiguously recognized as the chemical fossils of BHPs (35). Because BHPs with an extended side chain and 35 carbon atoms are known to be produced only by bacteria, extended C_{31} to C_{35} sedimentary

* Corresponding author. Mailing address: Department of Biology, 77 Massachusetts Ave., 68-380, Cambridge, MA 02139. Phone: (617) 324-2770. Fax: (617) 324-3972. E-mail: dkn@mit.edu.

† Supplemental material for this article may be found at http://jb.asm.org/.

▽ Published ahead of print on 10 July 2009.

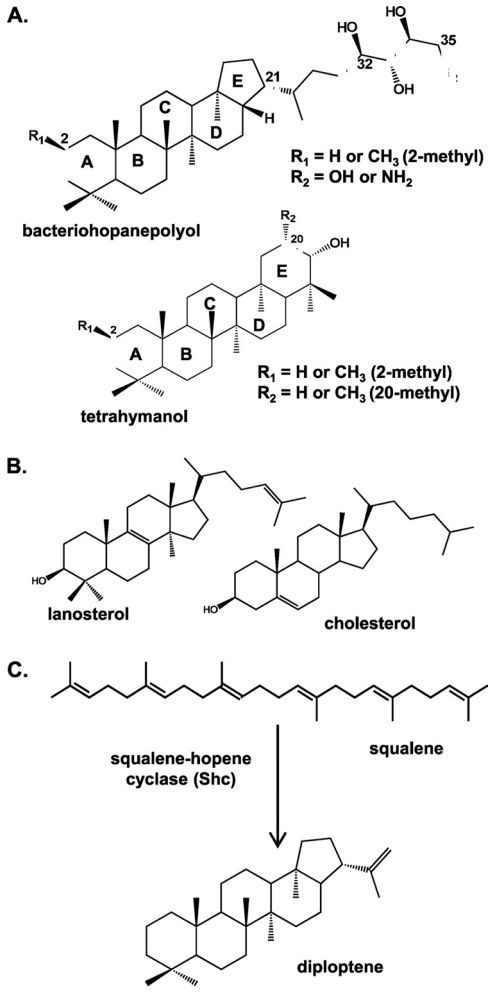

FIG. 1. Biosynthesis of hopanoids in *R. palustris* TIE-1. (A) Hopanoids produced by *R. palustris* TIE-1. For 32,33,34,35-bacteriohopanetetrol, R_2 is OH; for 35-amino-32,33,34-bacteriohopanetriol, R_2 is NH_2. (B) Structures of the sterol biosynthesis intermediate lanosterol and of cholesterol, demonstrating the structural similarity to hopanoids. (C) Conversion of squalene to the basic hopene structure by the squalene-hopene cyclase. The Entrez Gene accession number for the squalene-hopene cyclase gene is NC_011004.1.

hopanes are thought to be specific to this domain (34, 49). Furthermore, extended hopanes that are methylated at C-2 have been considered to be indicators of cyanobacteria, whereas C-3 methylated hopanes are thought to be diagnostic for microaerophilic methanotrophs and acetic acid bacteria (56, 64).

To date, no studies have addressed the function of hopanoids in geologically relevant organisms, such as photosynthetic bacteria. The use of hopanoids as biomarkers would be greatly enhanced if they could be attributed to specific bio(geo)chemical processes as opposed to their use solely as taxonomic proxies. Hopanoids are not produced by all bacteria, and their distribution among these groups does not appear to follow a systematic pattern (8, 49). Furthermore, specific sedimentary hopanes have been interpreted as biomarkers for certain metabolisms in modern microbes in the absence of direct experimental evidence linking the two. For example, BHPs methylated at C-2 were known to be produced in abundance by cyanobacteria, and taking this together with their prevalence in ancient marine petroleum source rocks, they were proposed as biomarkers not only for cyanobacteria, but also for oxygenic photosynthesis (49, 56). However, there is no evidence that functionally links 2-methylbacteriohopanepolyols (2-MeBHPs) with oxygenic photosynthesis in modern cyanobacteria. Furthermore, the lack of studies addressing the regulation of the production of hopanoids in modern bacteria limits our ability to constrain these molecules to a specific bacterial group. An example is the recent discovery of significant 2-MeBHP production by the anoxygenic phototroph *Rhodopseudomonas palustris*, which had been previously tested and was thought not to produce methylated hopanoids (31, 48). This demonstrated not only that organisms other than cyanobacteria are able to make 2-MeBHPs, but also that the production of these molecules depends on the growth conditions (48).

Given these ambiguities, there are inadequate data to fully interpret the sedimentary hopane record. To begin to understand the physiological functions of hopanoids in photosynthetic bacteria and to compare these functions to those of sterols in eukaryotes, we generated and characterized a hopanoid deletion mutant of the genetically tractable anoxygenic phototroph *R. palustris* TIE-1.

MATERIALS AND METHODS

Bacterial strains, media, and growth conditions. The bacterial strains used in this study are listed in Table 1. *Escherichia coli* strains were grown in lysogeny broth (LB) at 37°C. *E. coli* strain BW29427 was supplemented with 60 μM diaminopimelic acid. For aerobic chemoheterotrophic growth, *R. palustris* strains were grown in unbuffered YP medium (0.3% yeast extract, 0.3% peptone) at 30°C in the dark with shaking at 250 rpm. Buffered YP medium was prepared by adding 100 mM MES (4-morpholineethanosulfonic acid) for pH 4.5, 5, and 6; 100 mM MOPS (4-morpholionepropanesulfonic acid) for pH 7; or 100 mM bicine [*N*,*N*-bis(2-hydroxyethylglycine)] for pH 8 and pH 9 and adjusting the medium to the desired pH with concentrated HCl or NaOH prior to autoclaving it. For anaerobic phototrophic growth, *R. palustris* strains were grown in anaerobic bicarbonate-buffered freshwater (FW) medium (22). Unless otherwise noted, FW medium was supplemented from sterile anoxic stock solutions with 2 mM sodium acetate for photoheterotrophic growth and 2 mM sodium thiosulfate for photoautotrophic growth. All anaerobic cultures were flushed and pressurized to 5 lb/in^2 with N_2/CO_2 (80%/20%) and incubated at 30°C at 50 W/m^2 without shaking. For anaerobic photoheterotrophic growth at acidic and alkaline pH, FW medium was prepared without bicarbonate in the medium or CO_2 in the headspace to prevent fluctuations in the pH. Anoxic acidic medium was buffered with 50 mM MES, and alkaline medium was buffered with 50 mM HEPES [4-(2-hydroxyethyl)piperazine-1-ethanesulfonic acid], and the headspace was flushed with N_2 rather than N_2/CO_2. This medium was supplemented with 10 mM acetate, and the pH was adjusted both before and after autoclaving. For growth on solid medium, LB or YP was solidified with 1.5% agar and supplemented, if necessary, with gentamicin at 20 μg/ml (*E. coli*) or 800 μg/ml (*R. palustris*), kanamycin at 50 μg/ml (*E. coli*) or 400 μg/ml (*R. palustris*), spectinomycin at 100 μg/ml, or bile salts at 1.5%.

For growth curves and doubling-time calculations, exponential-growth-phase cells were inoculated in triplicate into the appropriate medium with a 1% inoculum and monitored for growth by following the increase in absorbance at 600 nm over time. Absorbance at 600 nm versus time was graphed on a log scale, and the slope of the curve was used to determine the growth rate constant, k. The doubling time, g, was calculated from the following equation: $g = \ln(2)/k$.

DNA methods, plasmid construction, and transformation. All plasmid constructions and primers used in this study are described in Table 1 and Table 2. A QIAprep Spin Miniprep Kit (Qiagen, Valencia, CA) was used for isolation of plasmid DNA from *E. coli*. Genomic DNA from *R. palustris* strains was isolated using the DNeasy Blood and Tissue Kit (Qiagen, Valencia, CA). DNA sequences of all cloning intermediates were confirmed by sequencing at the Biopolymers Laboratory in the Massachusetts Institute of Technology Center for Cancer Research. *E. coli* strains were transformed by electroporation using an Electro-

TABLE 1. Strains and plasmids used in this study

Strain or plasmid	Genotype, markers, or characteristics[a]	Source
Strains		
E. coli S17-1	*thi pro hdsR hdsM*$^+$ *recA*; chromosomal insertion of RP4-2 (Tc::Mu Km::Tn*7*)	53
E. coli BW29427	*thrB1004 pro thi rpsL hsdS lacZ*ΔM15 RP4-1360 Δ(*araBAD)567* Δ*dapA1341*::[*erm pir* (wt)]	W. W. Metcalf
R. palustris TIE-1	Isolated from Woods Hole, MA	22
R. palustris Δ*shc*	*R. palustris* TIE-1 Δ*shc*	This study
R. palustris Δ*shc*+pPVW8	*R. palustris* TIE-1 Δ*shc* transformed to Km^r with pPVW8	This study
Plasmids		
pJQ200SK	Mobilizable suicide vector; *sacB* Gm^r	46
pBBR1MCS-2	5.1-kb broad-host-range plasmid; Km^r *lacZ*	25
pCR8/GW/TOPO	2.8-kb TA cloning vector; Sp^r	Invitrogen, Carlsbad, CA
pPVW3	1-kb *shc* upstream region PCR amplified with primers PW13 and PW14 and cloned into pJQ200SK at NotI and SpeI	This study
pPVW4	1-kb *shc* downstream region PCR amplified with primers PW15 and PW16 and cloned into pJQ200SK at SpeI and XmaI	This study
pPVW6	NotI- and SpeI-cut *shc* upstream fragment from pPVW3 subcloned into pPVW4	This study
pPVW8	KpnI- and SpeI-cut 4-kb *shc* complementation fragment from pPVW23 subcloned into pBBR1MCS-2	This study
pPVW23	4-kb *shc* complementation fragment PCR amplified with primers PW25 and PW26 and cloned into pCR8/GW/TOPO	This study

[a] Gm, gentamicin; Km, kanamycin; Sp, spectinomycin.

porator 2510 (Eppendorf, Hamburg, Germany) as recommended by the supplier. Plasmids were mobilized from *E. coli* S17-1 or BW29427 into *R. palustris* by conjugation on YP agar plates that were incubated overnight at 30°C (23, 39).

Construction of an *R. palustris shc* deletion strain. The *shc* deletion strain was constructed in *R. palustris* TIE-1 as previously described (22, 23). Briefly, a deletion plasmid construct, pPVW6, was made by fusing 1 kb of the *shc* upstream region with 1 kb of the downstream region in the suicide vector pJQ200SK (46). pPVW6 was integrated onto the *R. palustris* TIE-1 chromosome through homologous recombination with either the *shc* upstream or downstream region. Because pJQ200SK contains a gentamicin resistance marker, as well as the *sacB* gene, the resulting *R. palustris* strain was both gentamicin resistant and sucrose sensitive (46). To remove the plasmid from the chromosome and generate the Δ*shc* mutant, one gentamicin-resistant colony was grown in YP broth without any antibiotic selection for 2 days. Because loss of pPVW6 from the chromosome restored sucrose resistance, serial dilutions were plated on YP agar supplemented with 10% sucrose. Several sucrose-resistant colonies were verified as deletion mutants by PCR (data not shown), and one Δ*shc* colony was picked for further characterization. A more detailed explanation of the method used to generate this mutant is presented in the supplemental material.

Complementation of the Δ*shc* strain. The *shc* gene plus 1 kb upstream and downstream of the gene was PCR amplified with primers PW25 and PW26 using the Failsafe PCR System. The 4-kb PCR fragment was cloned into the cloning vector pCR8.1 using the pCR8/GW/TOPO TA cloning kit (Invitrogen, Carlsbad, CA) and electroporated into *E. coli* DH10B. The complementation fragment was subcloned from pCR8.1 into pBBR1MCS-2, a cloning vector shown to self-replicate in *R. palustris* TIE-1 (23, 27). The resulting plasmid, pPVW8, was transformed into the *E. coli* mating strain BW29427 and mated into the Δ*shc* mutant strain on YP agar plates supplemented with diaminopimelic acid (23). Transformants were selected on YP agar containing 400 μg/ml kanamycin. Kanamycin-resistant colonies were screened for the presence of pPVW8 by PCR. All growth conditions included kanamycin at 400 μg/ml to maintain the plasmid in this strain.

Electron microscopy of *R. palustris* strains. *R. palustris* cultures were grown chemoheterotrophically as described above. Mid-exponential- and late-stationary-phase cultures were harvested by centrifugation (5,000 × *g* for 10 min) and washed twice in 50 mM HEPES buffer (pH 6.8). The cells were enrobed in 2% (wt/vol) Noble agar and placed in 2% glutaraldehyde for 2 h. The agar blocks were then washed twice in HEPES buffer and fixed in 2% osmium tetraoxide (OsO_4) for 2 h, followed by 2% (wt/vol) uranyl acetate staining for 2 h. The blocks were then dehydrated through a graded ethanol series (25%, 50%, 75%, 95%, and three times at 100%) for 15 min in each solution. The blocks were suspended in a 50/50 ethanol/LR White resin, a polyhydroxy-aromatic acrylic resin, solution for 30 min, followed by 100% LR White for 1 h. Samples were then embedded in gelatin capsules filled with fresh LR White resin, which was allowed to polymerize at 60°C for 1 h. The capsules were thin sectioned on a Reichert-Jung Ultracut E ultramicrotome, and ultrathin sections were mounted on Formvar carbon-coated copper grids. To improve contrast, the grids containing thin sections were poststained in 2% (wt/vol) uranyl acetate. Electron microscopy was performed on a Jeol JEM-1200EXII transmission electron microscope.

qRT-PCR. For exponential-phase versus stationary-phase assays, *R. palustris* TIE-1 was grown aerobically in 10 ml of unbuffered YP medium. All 10 ml of

TABLE 2. Primers used in this study

Primer	Sequence[a]	Restriction sites
PW13	GGCGCGCCGCGGCCGCGCGCTGGCGGCTGAAGCTCG	AscI/NotI
PW14	GGCGCGCCACTAGTTTTATCTGCTGTGTCTCCGT	AscI/SpeI
PW15	GGCGCGCCACTAGTTTCTGGGGGCAGTGGACGAC	AscI/SpeI
PW16	GGCGCGCCCCCGGGTCGTCGCGCCGAAGGAGTTC	AscI/XmaI
PW21	TTGGGGCGAAATCTGTAAAA	
PW22	TAATTCGTCGGTCAGTGCAA	
PW25	GAATTCGGTACCGCGATTACCTCGGCTTGAT	EcoRI/KpnI
PW26	GAATTCACTAGTGCGACCATCTGTTCGAAGG	EcoRI/SpeI
PW136	**TAATACGACTCACTATAGGGAGA**GCGCTGCTGAATTATCGTC	
PW137	CGACCAGCAAGAGATCAATG	
PW140	GTCGGCATCGACGAACTATT	
PW141	ATCCGAACAGCTTGAACAGC	

[a] Restriction sites are underlined; the T7 promoter is shown in boldface.

cells was transferred in mid-exponential phase (17 h after inoculation; optical density at 600 nm [OD_{600}], 0.1 to 0.2) or in late stationary phase (72 h after inoculation; OD_{600}, 0.3 to 0.4) into 2 volumes of RNAprotect Bacteria Reagent (Qiagen, Valencia, CA), incubated for 5 min at room temperature, and centrifuged for 20 min at 5,000 × *g*. RNA was extracted from the cell pellet using the RNeasy Mini Kit (Qiagen, Valencia, CA). Genomic DNA contamination was removed from each RNA sample with Turbo DNA-free DNase (Ambion, Foster City, CA). cDNA was generated from 100 ng of the extracted RNA with the iScript cDNA Synthesis Kit (Bio-Rad, Hercules, CA). The cDNA (2 μl) was then used as a template for quantitative PCR using the iTaq SYBR green Supermix with Rox (Bio-Rad, Hercules, CA) and primers PW140 and PW141, which are specific for the *shc* gene. All samples were assayed in triplicate, and the cycle time was determined automatically by the Real Time 7500 PCR software (Applied Biosystems, Foster City, CA). Primers (Integrated DNA Technologies, Coralville, IA) for quantitative reverse transcriptase (qRT) PCR were designed using Primer3 software (50) and are listed in Table 2.

For pH shock assays, *R. palustris* TIE-1 was grown either chemoheterotrophically in 100 ml of YP medium buffered at pH 7 with 100 mM MOPS or photoheterotrophically in 10 ml FW medium supplemented with 10 mM acetate (N_2 headspace) and buffered at pH 6.5 with 50 mM MES. For chemoheterotrophic assays, 50 ml of cells was removed in late stationary phase (72 to 96 h; OD_{600}, 0.3 to 0.4) and split into five tubes (10 ml/tube). The cells were centrifuged at 5,000 × *g* for 20 min at 4°C. The pellets were resuspended in 5 ml of sterile YP medium buffered with 100 mM MES (pH 5 and 6), 100 mM MOPS (pH 7), or 100 mM bicine (pH 8 and 9) and incubated for 30 min at 30°C in the dark with shaking. For photoheterotrophic assays, all treatments were done under anoxic conditions. Eight milliliters of stationary-phase cells (48 h; OD_{600}, 1.3 to 1.5) was split into four tubes (2 ml/tube) and centrifuged at 10,000 × *g* for 1 min at room temperature. The cells were resuspended in 2 ml of sterile anoxic FW medium buffered with 50 mM MES (pH 6.5) or 50 mM HEPES (pH 7.5, 8.0, or 8.5) and incubated for 30 min at 30°C in the light without shaking. After the pH shock incubation, both chemoheterotrophic and photoheterotrophic cells were immediately transferred to twice the cell volume of RNAprotect Bacteria Reagent (Qiagen, Valencia, CA), incubated for 5 min at room temperature, and centrifuged for 20 min at 5,000 × *g*. RNA extraction and qRT-PCR were performed as described above.

To generate a standard curve of the *shc* amplicon (12), an 847-bp fragment of the *shc* gene with the T7 promoter inserted at the 5′ end was amplified with primers PW136 and PW137. The PCR product was gel purified using the Qiagen Gel Extraction Kit (Qiagen, Valencia, CA), and 100 ng of the PCR product was used in the Megascript T7 Kit (Ambion, Foster City, CA) to generate an in vitro-transcribed sense RNA transcript. The transcription reaction mixture was treated with Turbo DNA-free DNase to remove any DNA template and further purified with the Megaclear Kit (Ambion, Foster City, CA) to remove unincorporated nucleoside triphosphates, enzymes, and buffer components. The concentration of each transcript was determined by averaging triplicate measurements of its concentration on a NanoDrop 1000 (Thermo Scientific, Waltham, MA). Assuming the average mass of a ribonucleotide was 340 Da, the concentration of each transcript was converted to copy numbers/μl, diluted to 2×10^{10} copies/μl, and stored at −80°C. The standard curve was generated by performing two independent 10-fold serial dilutions of the RNA standard and using 5 μl of each dilution in the reverse transcription reaction. Two microliters of the cDNA was used as a template for quantitative PCR using the *shc*-specific primers PW140 and PW141. A standard curve was generated by plotting cycle time values against the log of the initial copy number. The copy number of *shc* transcripts in each RNA sample was calculated after real-time amplification from the linear regression of the standard curve.

Total hopanoid quantification in *R. palustris* TIE-1. For comparison of hopanoid abundances in exponential versus stationary phase, *R. palustris* TIE-1 was grown under chemoheterotrophic and photoheterotrophic conditions. Cultures (1 liter) were harvested in log phase (17 h after inoculation; OD_{600}, 0.1 to 0.2) or stationary phase (72 to 96 h after inoculation; OD_{600}, 0.3 to 0.4 for chemoheterotrophic growth and 0.9 to 1.0 for photoheterotrophic growth) by centrifugation at 5,000 × *g* for 20 min at 4°C. The cells were washed once in 10 ml of unbuffered YP medium, and the cell pellets were frozen and lyophilized overnight.

For hopanoid quantification after pH shock, *R. palustris* TIE-1 was grown aerobically in YP medium (1 liter) buffered at pH 7 with 100 mM MOPS to late stationary phase (72 to 96 h; OD_{600}, 0.3 to 0.4); 900 ml of culture was removed and split into three centrifuge bottles (300 ml/bottle). The cells were centrifuged at 5,000 × *g* for 20 min at 4°C. The pellets were resuspended in 150 ml sterile YP medium buffered at pH 5 (100 mM MES), pH 7 (100 mM MOPS), or pH 9 (100 mM bicine) and incubated overnight with shaking at 30°C in the dark. The cells were pelleted at 5,000 × *g* for 20 min at 4°C and washed once with 10 ml of the appropriate YP medium (at pH 5, 7, or 9). The cell pellets were frozen and lyophilized overnight.

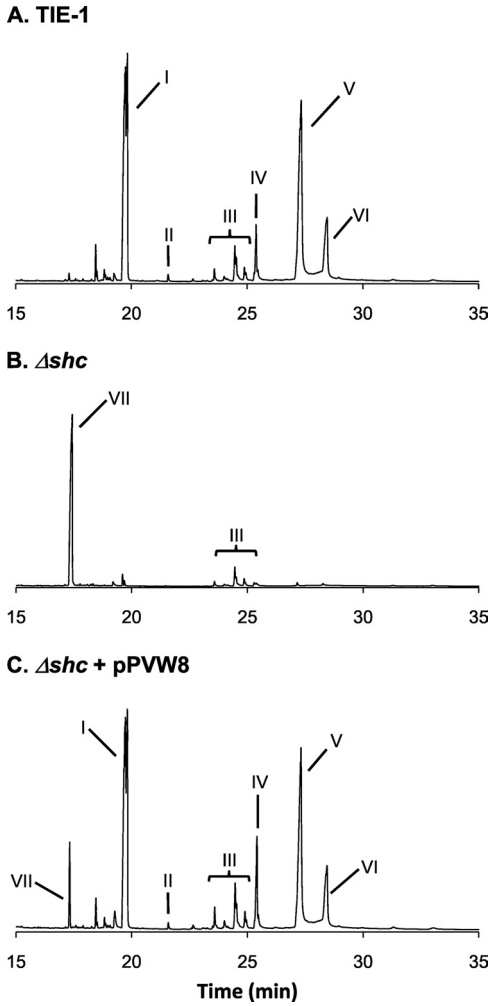

FIG. 2. GC-MS chromatograms of total lipid extracts from TIE-1 strains. (A) *R. palustris* TIE-1. (B) *R. palustris* Δ*shc*. (C) *R. palustris* Δ*shc* plus pPVW8. The numbered compounds are as follows: I, hopene (desmethyl and 2-methyl); II, tetrahymanol (desmethyl, 2-methyl, and 20-methyl); III, triglycerides; IV, unidentified BHP; V, bacteriohopanetetrol (desmethyl and 2-methyl); VI, aminobacteriohopanetriol; VII, squalene. Retention times for each compound are listed in Table S1 in the supplemental material. At this point, we have not identified compound IV, and it remains unclear whether this is a true hopanoid product of *R. palustris* TIE-1 or a degradation product of the high-temperature hopanoid analysis method.

GC-MS analysis. For initial hopanoid analysis of the Δ*shc* mutant (Fig. 2), cells were grown chemoheterotrophically in 250 ml YP to late stationary phase (5 days). The cells were harvested by centrifugation at 5,000 × *g* for 20 min at 4°C. The cell pellets were frozen and lyophilized overnight in a VirTis K-series freeze dryer (VirTis, Gardiner, NY). Lipids were extracted by sonicating the cells in Teflon centrifuge tubes (VWR, Bridgeport, NJ) for 15 min at room temperature in 10 ml of 10:5:4 methanol (MeOH)/dichloromethane (DCM)/water (5). Samples were centrifuged for 10 min at 3,000 × *g*, and the supernatant was transferred to a new tube. The cell pellets were sonicated again in 10 ml of MeOH/DCM/water and centrifuged, and the supernatant was combined with the first extraction. The samples were separated into two phases by adding 10 ml each of DCM and water and centrifuged for 10 min at 3,000 × *g*, and the organic phase was transferred to a new vial. To the remaining aqueous phase, 10 ml each of DCM and water was added again and centrifuged, and the organic phase was

again removed and combined with the previous extraction. This was repeated two more times for a total of four extractions. The total lipid extract was evaporated under N_2 and derivatized to acetate esters for gas chromatography/mass spectrometry (GC-MS) analysis by incubation in 100 μl of 1:1 acetic anhydride/pyridine for 1 h at 70°C. To suppress the decomposition of unstable compounds, the derivatized samples were injected directly into acetic anhydride/pyridine. For total hopanoid quantification in *R. palustris* TIE-1 (see Table 4), dry cells were weighed and then extracted by ultrasonication in a mixture of 10:5:4 MeOH/DCM/water (5). This total lipid extract was dried at room temperature under N_2, weighed, and redissolved in DCM. A 0.5-mg aliquot of the total lipid extract was taken for GC-MS analysis, and an internal standard (7 μg epiandrostanol) was added. This mixture was acetylated by heating it with acetic anhydride/pyridine at 80°C for 15 min.

The lipid extracts were analyzed by GC-MS, and we employed a novel protocol for high-temperature GC-MS analysis that allowed functionalized BHPs to be directly analyzed. For the initial analysis of the Δ*shc* mutant (Fig. 2), lipid extracts were separated on a Hewlett-Packard 6890 series gas chromatograph equipped with a DB1-HT column (15 m by 0.25 mm [inside diameter] by 0.1-μm film thickness) with helium as the carrier at a constant flow of 1 ml/minute and programmed as follows: 80°C for 2 min, ramped 10°C /minute to 360°C, and held 20 min. One microliter of the sample was injected into a Gerstel programmable temperature vaporization injector operated in splitless mode at 80°C and programmed to 360°C at 720°C/minute, where it was held for the duration of the run. The gas chromatograph was coupled to a 5975 series MSD (mass selective detector) with the source at 200°C and operated at 70 eV in EI (electron ionization) mode scanning from 50 to 850 Da in 0.5 s.

For total hopanoid quantification of *R. palustris* TIE-1 (see Table 4), lipid extracts were separated on a Thermo Scientific TraceGC. Samples were injected into a programmable temperature vaporization injector operated in splitless mode at 60°C with a 2-mm (inside diameter) deactivated glass liner and programmed to 325°C for the duration of the run. A DB-XLB column (30 m by 0.25 mm by 0.10-mm film thickness) was employed and was temperature programmed from 100 to 350°C, holding 15 min at the maximum temperature. The GC was coupled to a Thermo DSQ mass spectrometer with the source at 220°C and operated at 70 eV in EI mode scanning from 50 to 750 Da in 0.3 s. Using this program, bacteriohopanetetrol acetate eluted in approximately 38 min, while the desmethyl and 2-methyl homologs remained chromatographically resolved. We did not observe the bacteriohopaneaminotriol using this method and column, although its presence was detected using the DB-1HT GC-MS method described above and has been previously observed by liquid chromatography-MS analyses (48).

Compounds were identified by comparison of retention times and mass spectra to those of authentic compounds (tetrahymanol from *Trimyema* sp., diplopterol from *Methylococcus capsulatus*, and bacteriohopanepentol from *M. capsulatus*) and published mass spectra (hopenes [55] and tetrahymanol [60]). Retention times and molecular ions are listed in Table S1 in the supplemental material. Methylation at C-2 was confirmed for bacteriohopanetetrol by comparison of mass spectra and retention times with those from *Phormidium luridum* (48). For all other compounds, C-2 methylation was inferred from the shift of fragments with *m/z* 191 to 205 and *m/z* 369 to 383 and from the relative retention time compared to the desmethyl homolog (~0.15 min earlier). Concentrations and 2-methyl/desmethyl ratios were calculated by comparing total ion chromatogram peak areas between the analytes and the internal standard and assuming identical response factors. This assumption was required because no pure standards are available for these compounds.

RESULTS

A squalene-hopene cyclase deletion mutant in *R. palustris* TIE-1 does not produce hopanoids. To better understand the physiological role of hopanoids in photosynthetic bacteria, we constructed a deletion mutant in *R. palustris* TIE-1 that no longer produced any hopanoids. A key step in the biosynthesis of hopanoids is the cyclization of squalene to the basic hopene structure, diploptene (Fig. 1C) (26). This reaction is catalyzed by the squalene-hopene cyclase, which is encoded by the *shc* gene (42). Utilizing the genomic data available from the *R. palustris* TIE-1 genome, we identified and made an in-frame deletion of the *shc* gene in this organism. The resulting Δ*shc* mutant accumulated a significant amount of squalene and did not produce any hopanoids, nor did it produce the triterpenoid tetrahymanol (Fig. 2). As can be seen in Fig. 1A, tetrahymanol differs from the hopanoids in having a six-membered E ring and no functionalized side chain. Previous in vitro characterization of the Shc protein from *R. palustris* demonstrated that the enzyme was able to convert squalene to diploptene but not to tetrahymanol (26). For that reason, it was presumed that another cyclase was involved in tetrahymanol biosynthesis. However, the deletion of *shc* in *R. palustris* showed that the Shc protein is indeed required to form this pentacyclic triterpenoid in vivo.

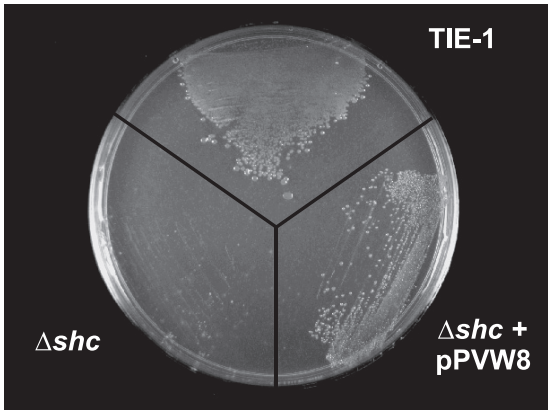

FIG. 3. Δ*shc* cells are more permeable to bile salts. The Δ*shc* strain is unable to grow in the presence of bile salts (1.5%), while both the wild type and the Δ*shc* complemented strain (Δ*shc*+pPVW8) are resistant.

To verify that the deletion of *shc* was responsible for the loss of hopanoid production, a copy of the TIE-1 *shc* gene was introduced into the Δ*shc* mutant on a self-replicating plasmid. Although the complemented (Δ*shc*+pPVW8) strain still accumulated squalene, the strain was now able to produce all of the known *R. palustris* hopanoids (Fig. 1A and 2). Therefore, the lack of hopanoid production in the Δ*shc* strain was due only to the deletion of *shc*.

Lack of hopanoids results in increased membrane permeability. Because hopanoids have been shown to localize to the inner and outer membranes of some bacteria (21, 24, 54), we hypothesized that a lack of hopanoids might lead to membrane damage in *R. palustris.* A strong indicator of outer membrane damage and permeability in gram-negative bacteria is sensitivity to bile salts and certain antibiotics (2, 51). As seen in Fig. 3, growth of the Δ*shc* mutant was inhibited in the presence of bile salts, while growth of the wild type and complemented strains was not. The mutant strain is also sensitive to the antibiotics erythromycin and rifampin (rifampicin), both inhibitors of protein synthesis (51). The Δ*shc* strain had a 7-mm zone of inhibition with erythromycin, while both TIE-1 and the complemented strain were resistant to the antibiotic (data not shown). The wild-type strain did display some sensitivity to rifampin, with a zone of inhibition of 5 mm. However, the zone of inhibition in the deletion strain increased to 10 mm, indicating that the lack of hopanoids increased sensitivity (data not shown). Together, these data demonstrate that hopanoids may be important in decreasing membrane permeability and, like

TABLE 3. Doubling times of the *R. palustris* Δ*shc* strain under various growth conditions

Growth condition[a]	Doubling time (h)[b]	
	R. palustris TIE-1	*R. palustris* Δ*shc*
Chemoheterotrophic	3.8 ± 0.1	4.1 ± 0.1
Photoheterotrophic	6.1 ± 0.2	7.6 ± 0.7
Photoautotrophic	8.0 ± 0.2	9.0 ± 0.3

[a] See Materials and Methods for detailed growth conditions.
[b] Growth rates were measured by monitoring the OD_{600} during growth, and the doubling times were calculated from three replicate cultures. Each value represents the average and standard deviation of three biological replicates grown under identical conditions.

sterols in eukaryotes, may play a role in maintaining membrane integrity.

Hopanoids are important in the stationary phase of chemoheterotrophic growth. The Δ*shc* mutant was able to grow on all growth substrates tested. Although photoautotrophic and photoheterotrophic growth were slightly slower in the Δ*shc* mutant than in the wild-type strain (Table 3), the deletion strain was still able to achieve the same final OD. Thus, hopanoids are not required for photosynthesis in *R. palustris*.

The growth rate during aerobic chemoheterotrophic growth was the same in the deletion mutant as in the wild-type strain (Table 3). However, a significant drop in OD was observed when cells entered stationary phase during chemoheterotrophic growth (Fig. 4A). Transmission electron microscopy images of both the wild type and deletion mutant illustrated that the Δ*shc* strain was severely damaged in stationary phase but not in exponential phase (Fig. 4C and D). This morphological defect in stationary phase may explain the observed drop in OD.

The Δ*shc* mutant is sensitive to alkaline conditions. Several studies with *E. coli* have demonstrated that the pH of rich media, such as LB or YP, increases in stationary phase (11). We reasoned that the drop in OD and the morphological damage seen in stationary phase for the Δ*shc* mutant might be due to an increase in pH. We measured the pH of the growth medium at the beginning and end of chemoheterotrophic growth and found that the pH had increased from 7.2 to 8.2 for

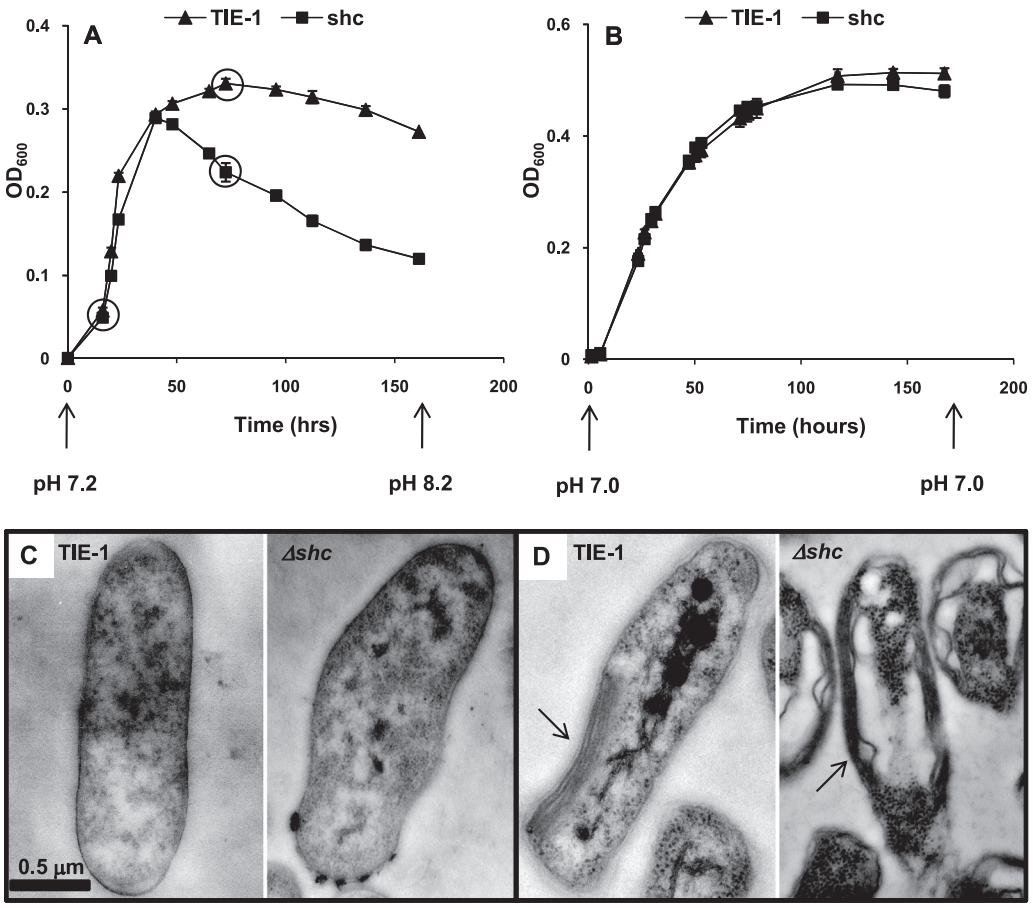

FIG. 4. Δ*shc* chemoheterotrophic growth and morphology. (A) Chemoheterotrophic growth of TIE-1 and the Δ*shc* strain in unbuffered medium (A) or buffered medium (B) at pH 7. Each time point represents the average of three replicate cultures (the error bars represent standard deviations and may not be visible beneath the data point markers). Each growth curve was repeated at least three times, and representative growth curves are shown. The circled points in panel A indicate when cultures were harvested for transmission electron microscopy. (C) Transmission electron microscopy of chemoheterotrophically grown TIE-1 and Δ*shc* cells harvested during mid-exponential growth (17 h after inoculation). (D) Transmission electron microscopy of chemoheterotrophically grown TIE-1 and Δ*shc* cells harvested during stationary phase (72 h after inoculation). The arrows indicate the formation of the inner cytoplasmic membrane (lamellar membrane) as anoxic phototrophic growth was induced.

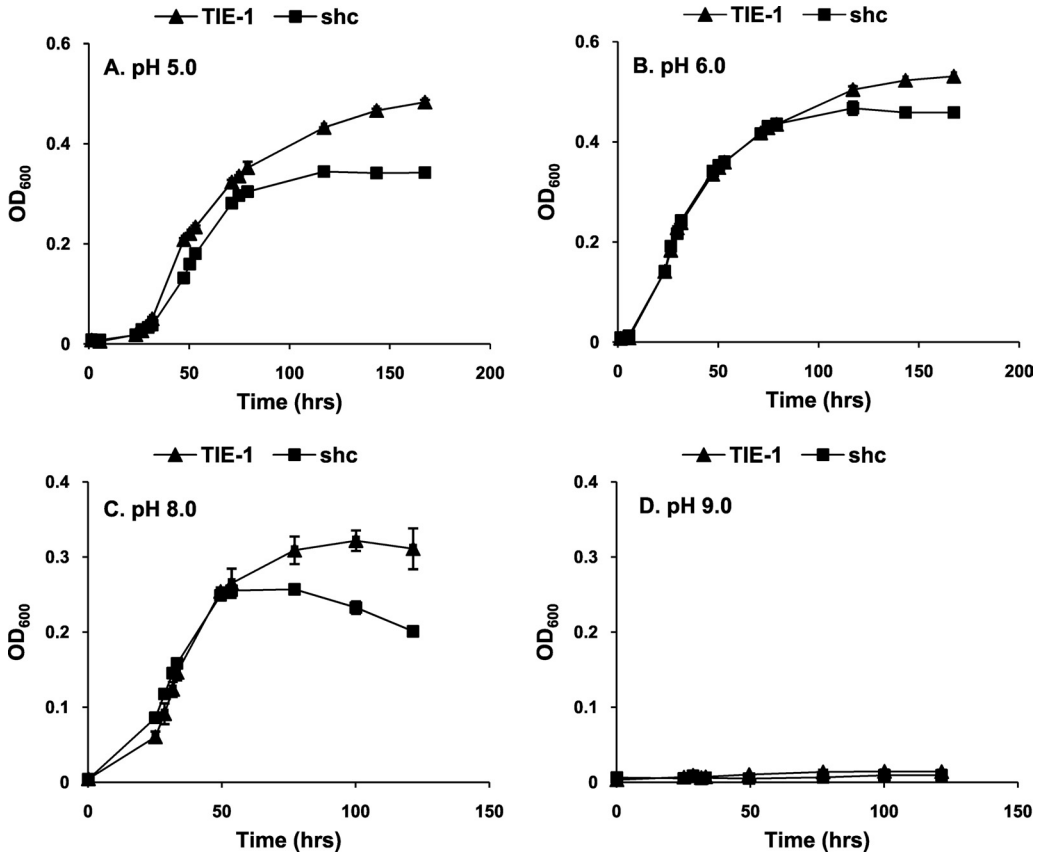

FIG. 5. pH effect on Δ*shc* chemoheterotrophic growth. Shown are chemoheterotrophic growth curves of the TIE-1 and Δ*shc* strains in YP medium buffered at pH 5 (A), pH 6 (B), pH 8 (C), and pH 9 (D). Each time point represents the average of three replicate cultures (the error bars represent standard deviations and may not be visible beneath the data point markers). Each growth curve was repeated at least three times, and representative growth curves are shown.

both TIE-1 and Δ*shc* (Fig. 4A). The growth experiment was repeated in YP medium buffered with 100 mM MOPS at pH 7. In the buffered medium, the pH remained constant throughout the growth curve and the drop in OD observed in unbuffered medium no longer occurred (Fig. 4B). This indicated that the growth defect of the Δ*shc* mutant in stationary phase was related to the increase in pH.

To determine if the drop in OD observed in the Δ*shc* mutant was specific to stationary-phase cells and alkaline conditions, both strains were grown in YP medium buffered at pH 4.5, 5, 6, 8, or 9. Because the medium was buffered, the pH should have remained constant throughout growth and the cells would have experienced either acidic or alkaline stress. Neither the wild type nor the mutant was able to grow at pH 9 (Fig. 5) or at pH 4.5 (see Fig. S1 in the supplemental material). Both strains were able to grow at pH 5, 6, and 8, but the Δ*shc* mutant had a growth defect at pH 5 and pH 8 (Fig. 5). Taken together, these data indicate that the wild type may be sensitive to both acidic and alkaline stress and that the decreased membrane permeability of the Δ*shc* mutant may aggravate this sensitivity. Interestingly, the growth of the Δ*shc* mutant was similar to that of the wild type during exponential phase under each pH tested. It was primarily during stationary phase that the behavior of the strains deviated from one another, particularly at pH 8. Hopanoids thus seem to be most relevant in protecting stationary-phase cells from pH stress.

pH stress inhibits phototrophic growth in the Δ*shc* mutant. The high cell density of stationary-phase cultures often results in oxygen-limiting conditions (45). Given that oxygen limitation stimulates the transition from aerobic chemoheterotrophic growth to anaerobic phototrophic growth in *R. palustris* (7), it seemed likely that chemoheterotrophically grown TIE-1 cells in stationary phase were switching from oxic growth to anoxic growth. This was confirmed by the presence of photosynthetic lamellar membranes, whose development is stimulated by oxygen deprivation (7), in stationary-phase TIE-1 cells but not in exponential-phase cells (Fig. 4C and D). Therefore, we hypothesized that the acidic and alkaline growth defect observed primarily in stationary-phase Δ*shc* cells may have been related to phototrophic growth. To test this, we grew Δ*shc* and TIE-1 cells photoheterotrophically in 10 mM acetate buffered with 50 mM MES at pH 4.5, 5.0, 5.5, and 6.0 and buffered with 50 mM HEPES at pH 6.5, 7.5, 8, and 8.5.

Both the wild type and the Δ*shc* strain were unable to grow at pH 5.0 or lower (see Fig. S2 in the supplemental material), but the wild-type strain was able to grow to a maximum OD_{600} of 1.5 when grown at pH 5.5 or higher (Fig. 6). Wild-type cells grown at pH 6.0, pH 8.0, and pH 8.5 exhibited an extensive lag

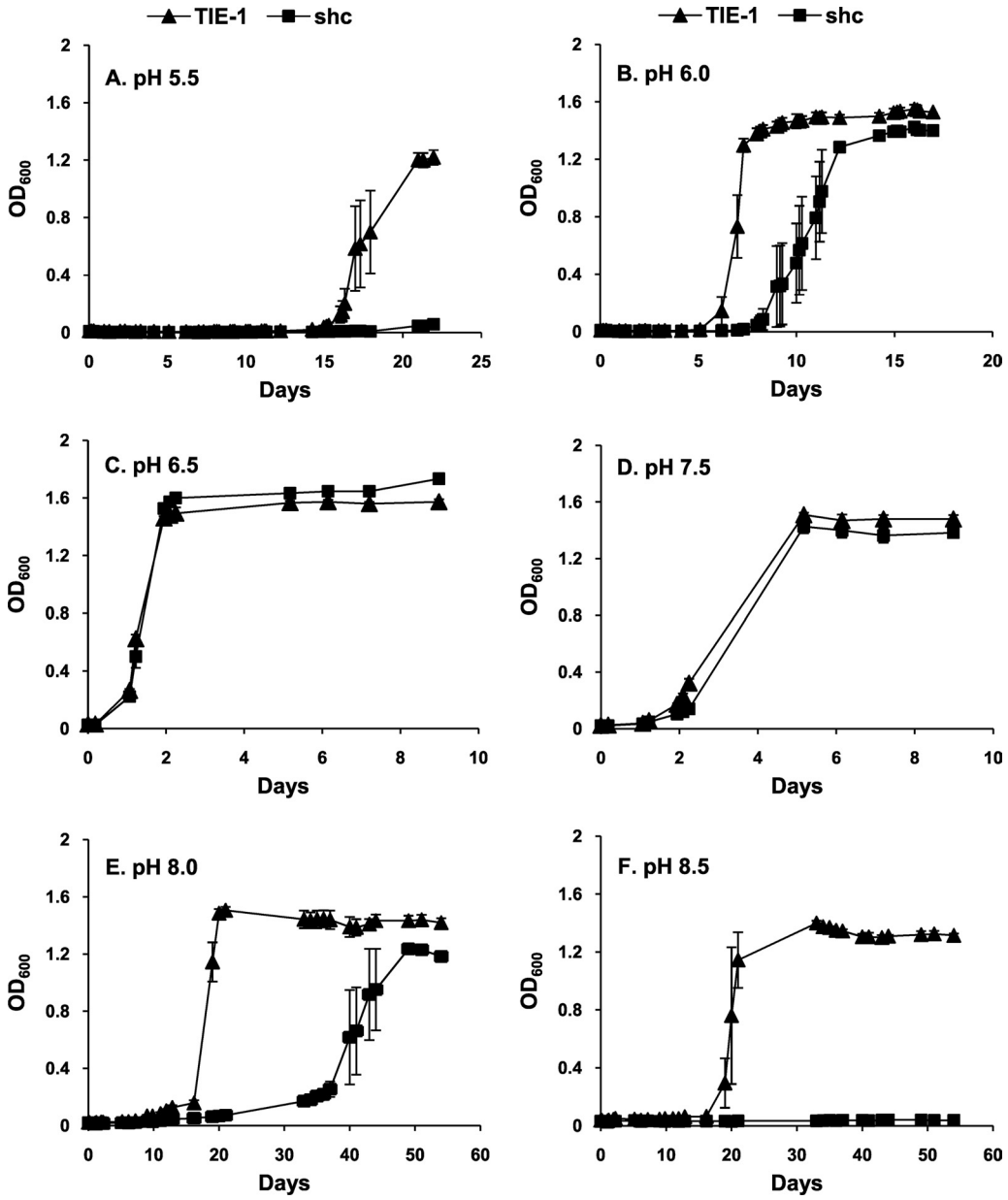

FIG. 6. pH effect on Δ*shc* photoheterotrophic growth. Shown is photoheterotrophic growth of TIE-1 and Δ*shc* strains in FW plus HEPES or FW plus MES medium supplemented with 10 mM sodium acetate under an N_2 headspace buffered at pH 5.5 (A), pH 6.0 (B), pH 6.5 (C), pH 7.5 (D), pH 8.0 (E), and pH 8.5 (F). Each time point represents the average of three replicate cultures, and the error bars represent standard errors. Each growth curve was repeated at least three times, and representative growth curves are shown.

phase compared to growth at pH 6.5 or 7.5, indicating that wild-type cells grown photoheterotrophically, like cells grown chemoheterotrophically, were also sensitive to both acidic and alkaline conditions. While the Δ*shc* strain had growth characteristics similar to those of the wild type at pH 6.5 and 7.5, the mutant strain had a much longer lag phase at pH 6.0 and pH 8.0 and did not grow at pH 5.5 or pH 8.5 (Fig. 6). Therefore, while hopanoids are not required for photosynthetic growth at neutral pH, these data indicate that they are required for photosynthetic growth at acidic or alkaline pH.

Transcription of the *shc* gene is minimally affected by pH shock. Given that hopanoids play a role in protecting TIE-1 cells against exposure to high and low pH, we sought to determine whether this role was regulated in response to pH. If hopanoids were specifically required for coping with alkaline stress in stationary phase, we hypothesized that transcription of the *shc* gene would be upregulated during stationary phase in unbuffered medium. To test this, TIE-1 cells were grown chemoheterotrophically in unbuffered YP medium and RNA was isolated from samples taken during exponential phase (17 h; pH ~7) and stationary phase (72 h; pH ~7.8). qRT-PCR was used to measure *shc* transcript levels in stationary-phase cells relative to log-phase cells, with a change in transcript levels greater than 2-fold or less than 0.5-fold considered significant.

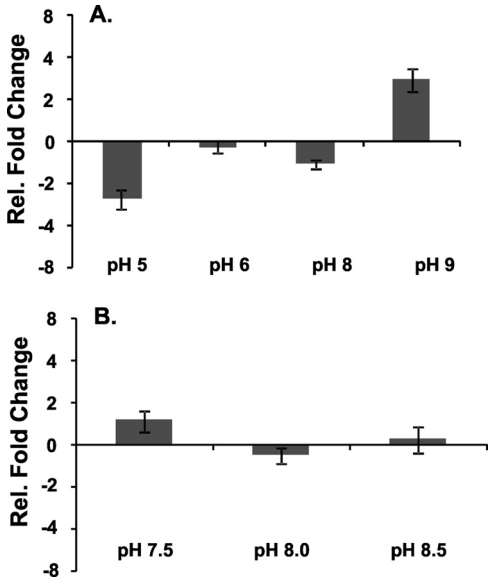

FIG. 7. pH effect on *shc* expression. qRT-PCR was used to measure the expression levels of the *shc* gene after pH shock. (A) Chemoheterotrophically grown cells (pH 7) were incubated in YP medium buffered at pH 5, 6, 7, 8, or 9 for 30 min. (B) Photoheterotrophically grown cells (pH 6.5) were incubated in FW medium buffered at pH 6.5, 7.5, 8.0, or 8.5 for 30 min. The transcript levels of *shc* were determined for each sample as described in Materials and Methods. Each data bar represents the change in transcript levels at the indicated pH relative to the pH 7 sample (A) or the pH 6.5 sample (B). The change was graphed on a $\log_2$ scale, and a change greater than 2 or less than 0.5 was considered significant. Each data point represents the average of biological triplicates, and the error bars represent standard errors.

Although the Δ*shc* mutant exhibited a severe growth phenotype in stationary phase, transcription of the *shc* gene did not increase in stationary phase but rather remained constant, with an average change in expression of 0.7- ± 0.2-fold (data not shown).

To determine if pH stress would increase the expression of *shc*, transcript levels of *shc* were also measured after TIE-1 cells had been shocked with acidic or alkaline medium. TIE-1 cells were grown chemoheterotrophically (buffered at pH 7) or photoheterotrophically (buffered at pH 6.5) to stationary phase. The cells were then shocked for 30 min in the same medium buffered at acidic, neutral, or alkaline pH. qRT-PCR was used to measure *shc* transcript levels under each shock condition relative to the neutral-pH incubation. As shown in Fig. 7A, we observed slight shifts in *shc* expression when chemoheterotrophically grown cells were shocked at pH 5 and 9. However, we did not observe any significant changes in *shc* expression under any pH shock condition for photoheterotrophically grown cells (Fig. 7B).

Total hopanoid production is not regulated by growth phase or pH. There are several possible reasons why increases in *shc* transcript levels during stationary phase or pH shock might not be physiologically important. First, the *shc* gene may be regulated posttranscriptionally, which qRT-PCR cannot detect. Alternatively, the *shc* gene may be constitutively expressed, which would prevent significant changes in transcript levels from one condition to another. If this were correct, then we would expect to see similar amounts of hopanoids produced under all conditions. To test this, the total hopanoid content was quantified in chemoheterotrophically and photoheterotrophically grown TIE-1 cells harvested during log phase and stationary phase, as well as cells incubated overnight under acidic or alkaline conditions.

Consistent with the qRT-PCR data, similar amounts of hopanoids were produced during log phase and stationary phase of chemoheterotrophic and photoheterotrophic growth (Table 4). We observed a significant increase in methylation at the C-2 position during stationary phase under both growth conditions (Table 4, 2-Me). A similar result was seen when chemoheterotrophically grown cells were transferred to alkaline pH. The amounts of hopanoids produced were the same under each pH; however, methylation at C-2 increased when the cells were subjected to alkaline conditions. In particular, methylation of one subset of hopanoids, the bacteriohopanetetrols, increased more than twofold at pH 9 compared to incubation at pH 7. These data, along with the qRT-PCR data, indicate that *shc* is constitutively expressed. Furthermore, these data suggest that the modification of hopanoids, such as methylation at C-2, changes in response to growth conditions.

DISCUSSION

Although hopanoids have been hypothesized to be sterol analogs in bacteria, the true physiological roles of these molecules have received little direct attention. A few studies have proposed that hopanoids are necessary for maintaining membrane integrity, as well as coping with external stresses, such as ethanol tolerance in *Z. mobilis* (19), oxygen diffusion in *Frankia* sp. (4), and prevention of water diffusion into *Streptomyces* spores (44). In vivo genetic studies with *Bacillus subtilis* have shown that sporulenes, polycyclic terpenoids similar to hopanoids, may be important in alleviating oxidative stress in spores (6). However, no in vivo genetic studies have been used to address the function of hopanoids in any strain, much less photosynthetic bacteria, which are of special interest to geobiologists. Given the ubiquity and abundance of hopanes in the rock record and their role as organic proxies for ancient bacterial life and metabolism, particularly oxygenic photosynthesis, it is important to understand how these molecules are used

TABLE 4. Hopanoid production and methylation at C-2 by *R. palustris* TIE-1

Growth condition[a]	Total hopanoids[b]		Bacteriohopanetetrol[b]	
	μg/mg dry biomass	% 2-Me	μg/mg dry biomass	% 2-Me
Chemoheterotrophic				
Exponential	25.3 ± 5.3	6.3 ± 0.9	3.4 ± 0.7	0.1 ± 0.1
Stationary	23.1 ± 7.1	20.0 ± 0.7	3.0 ± 1.4	3.4 ± 0.6
Photoheterotrophic				
Exponential	36.7 ± 1.6	47.1 ± 1.5	10.2 ± 0.6	9.8 ± 0.5
Stationary	34.2 ± 3.1	65.1 ± 3.2	8.2 ± 1.3	24.6 ± 5.9
pH shock				
pH 5	20.8 ± 2.6	50.7 ± 1.2	1.8 ± 0.5	6.1 ± 3.3
pH 7	27.3 ± 4.5	47.3 ± 2.8	3.3 ± 0.5	5.9 ± 0.9
pH 9	27.7 ± 0.9	54.4 ± 1.8	2.6 ± 0.4	13.3 ± 0.8

[a] See Materials and Methods for detailed growth and assay conditions.
[b] Each value represents the average and standard error of three biological replicates grown under identical conditions. 2-Me, 2-methyl.

by photosynthetic bacteria. Therefore, we set out to determine the physiological role of hopanoids in the genetically tractable anoxygenic phototroph *R. palustris* TIE-1.

Deletion of the squalene-hopene cyclase gene in *R. palustris* TIE-1 resulted in a strain that no longer produced any hopanoids. Physiological studies of the Δ*shc* mutant revealed that hopanoids are not required for growth in *R. palustris* TIE-1, as the mutant had growth characteristics similar to those of the wild type under standard chemoheterotrophic, photoautotrophic, and photoheterotrophic conditions. This demonstrates that hopanoids are not directly involved in anoxygenic photosynthesis and suggests that they may not be appropriate biomarkers for photosynthesis more generally.

The sensitivity of the Δ*shc* mutant to acidic and alkaline conditions was unexpected, given that *R. palustris* TIE-1 was isolated from an iron-rich mat located in a marsh with a pH range of 6 to 7 (22). Because the majority of *R. palustris* strains have been isolated from freshwater marsh sediments, it seems unlikely that hopanoid production evolved in these organisms as a mechanism to overcome pH stress (32, 33). This is consistent with our finding that hopanoid production is not regulated by acidic or alkaline conditions. Total hopanoid production remained constant when TIE-1 cells were exposed to high pH, either during stationary-phase growth or when they were shocked for a short time. If hopanoid production is not directly affected by pH stress, then what role might these molecules play in helping TIE-1 survive under acidic or alkaline conditions?

Studies of *E. coli* have demonstrated that acidic and alkaline exposure induces heat shock and SOS cellular responses, showing that extreme pH can be stressful for bacteria (13, 29, 52, 58, 63). The main effect of exposure to high or low pH is an immediate shift in the cytoplasmic pH, which the cell must readjust to maintain the optimal function and integrity of cytoplasmic proteins (37, 62). Several studies have revealed that cells are able to buffer their cytoplasmic pH immediately through the use of sodium/proton antiporters, symporters, and efflux pumps that transport protons in and out of the cytoplasm and, as a result, adjust the pH to more favorable conditions (10, 15, 28, 38).

Because cations and protons play important roles in alleviating acidic and alkaline stress, it is plausible that some bacterial cells have developed secondary mechanisms to prevent the accidental loss of protons and other cations. In particular, alkaliphilic *Bacillus* spp. have been shown to produce secondary wall polymers that associate with the peptidoglycan layer and presumably are able to bind cations and enhance their availability for pH homeostasis (1, 14). These bacteria also have high levels of squalene in their membranes, and it has been proposed that the high levels of this lipid might lower the permeability of protons across the lipid bilayer (18).

Interestingly, this same role has been put forward for both hopanoids in bacteria and sterols in eukaryotes (17). It has been proposed that both sterols and hopanoids may be able to pack the hydrophobic centers of lipid bilayers, preventing the loss of protons as charged water (17). Therefore, hopanoids may have an indirect but critical function in extreme-pH tolerance by preventing the unintentional loss of cations and protons across the inner and outer membranes. If this is true, then we might expect the lack of hopanoids to result in leaky membranes, making antiporters and overall pH homeostasis less efficient. The transmission electron microscopy images of the Δ*shc* mutant (Fig. 4C and D), together with its sensitivity to bile salts and specific antibiotics, imply that the membranes of the Δ*shc* mutant are damaged. Because the wild type is already somewhat sensitive to acidic and alkaline conditions, the increased membrane permeability resulting from the lack of hopanoids in the Δ*shc* mutant likely exacerbates this sensitivity. It remains unclear why this would affect phototrophically grown cells more than chemoheterotrophically grown cells. Because phototrophic growth induces the production of lamellar membranes for photosynthesis (7), under these growth conditions, more membranes are present. It is conceivable that more protons and cations might leak in the hopanoid mutant during phototrophic growth simply because there is a larger membrane area. Under these conditions, antiporters might be even less efficient, and the cell would be unable to neutralize its cytoplasm, which would result in impaired growth.

The constitutive expression of *shc* shows that hopanoids are produced under all growth conditions. It is interesting that while the total amount of hopanoids produced remains constant, the percentage of hopanoids methylated at C-2 increases significantly as cells shift from exponential to stationary phase, as well as in response to pH shock (Table 4). This suggests that it may be how hopanoids are modified rather than their total abundance that is important when bacteria encounter environmental stress. This agrees with what has been proposed for other hopanoid-producing bacteria. In *A. acidocaldarius*, a thermophilic acidophile, it was found that increasing temperature and decreasing pH did not alter the total amount of hopanoids produced, but production was shifted toward hopanoids with extended side chains (43). In *Frankia* sp., hopanoids were localized primarily to the nitrogenase vesicle; however, nitrogen-depleted conditions did not result in increased hopanoid production. It was speculated that nitrogen limitation causes hopanoids to congregate in the nitrogenase vesicle (4, 30).

In summary, our data suggest that hopanoids, like sterols, may be important in maintaining membrane integrity and for modulating membrane permeability. However, we do not yet know whether these effects are direct or indirect. It is possible that the lack of hopanoids altered the membrane architecture and/or the membrane protein content of the Δ*shc* mutant and that the phenotypes we observed resulted from these effects. Furthermore, our study did not distinguish which cyclic triterpenoids might be important for membrane permeability. Because *R. palustris* produces a variety of hopanoid molecules, as well as tetrahymanol, more work is needed to address how methylation and side chain modifications of the core hopanoid structure affect the functions of these molecules in *R. palustris* and other hopanoid-producing bacteria. These and other aspects of the cell biology of hopanoids will be the subjects of our future research.

ACKNOWLEDGMENTS

This work was supported by grants from the NASA Exobiology Program to A.L.S., D.K.N., and R.E.S. and an NSF Postdoctoral Minority Fellowship to P.V.W. D.K.N. is an Investigator of the Howard Hughes Medical Institute.

We thank David Doughty and Alex Poulain for comments on the manuscript and members of the Newman laboratory for helpful discussions.

REFERENCES

1. **Aono, R., and M. Ohtani.** 1990. Loss of alkalophily in cell wall component defective mutants derived from alkalophilic *Bacillus* C-125. Isolation and partial characterization of the mutants. Biochem. J. **266:**933–936.
2. **Begley, M., C. G. Gahan, and C. Hill.** 2005. The interaction between bacteria and bile. FEMS Microbiol. Rev. **29:**625–651.
3. **Benz, R., D. Hallmann, K. Poralla, and H. Eibl.** 1983. Interaction of hopanoids with phosphatidylcholines containing oleic and omega cyclohexyldodecanoic acid in lipid bilayer membranes. Chem. Phys. Lipids **34:**7–24.
4. **Berry, A. M., O. T. Harriott, R. A. Moreau, S. F. Osman, D. R. Benson, and A. D. Jones.** 1993. Hopanoid lipids compose the *Frankia* vesicle envelope, presumptive barrier of oxygen diffusion to nitrogenase. Proc. Natl. Acad. Sci. USA **90:**6091–6094.
5. **Bligh, E. G., and W. J. Dyer.** 1959. A rapid method for total lipid extraction and purification. Can. J. Biochem. Physiol. **37:**911–917.
6. **Bosak, T., R. M. Losick, and A. Pearson.** 2008. A polycyclic terpenoid that alleviates oxidative stress. Proc. Natl. Acad. Sci. USA **105:**6725–6729.
7. **Braatsch, S., J. R. Bernstein, F. Lessner, J. Morgan, J. C. Liao, C. S. Harwood, and J. T. Beatty.** 2006. *Rhodopseudomonas palustris* CGA009 has two functional *ppsR* genes, each of which encodes a repressor of photosynthesis gene expression. Biochemistry **45:**14441–14451.
8. **Brocks, J. J., and A. Pearson.** 2005. Building the biomarker tree of life, p. 233–258. *In* J. E. Banfield, J. Cervini-Silva, and K. H. Nealson (ed.), Molecular geomicrobiology. Reviews in mineralogy and geochemistry vol. 59. Mineralogical Society of America, Chantilly, VA.
9. **Brocks, J. J., and R. E. Summons.** 2004. Sedimentary hydrocarbons, biomarkers for early life, p. 63–115. *In* W. H. Schlesinger (ed.), Treatise on geochemistry, vol. 8. Elsevier-Pergamon, Oxford, United Kingdom.
10. **Cotter, P. A., V. Chepuri, R. B. Gennis, and R. P. Gunsalus.** 1990. Cytochrome *o* (*cyoABCDE*) and *d* (*cydAB*) oxidase gene expression in *Escherichia coli* is regulated by oxygen, pH, and the *fnr* gene product. J. Bacteriol. **172:**6333–6338.
11. **Farrell, M. J., and S. E. Finkel.** 2003. The growth advantage in stationary-phase phenotype conferred by *rpoS* mutations is dependent on the pH and nutrient environment. J. Bacteriol. **185:**7044–7052.
12. **Fey, A., S. Eichler, S. Flavier, R. Christen, M. G. Hofle, and C. A. Guzman.** 2004. Establishment of a real-time PCR-based approach for accurate quantification of bacterial RNA targets in water, using *Salmonella* as a model organism. Appl. Environ. Microbiol. **70:**3618–3623.
13. **Foster, J. W.** 2000. Microbial responses to acid stress, p. 99–115. *In* G. Storz and R. Hengge-Aronis (ed.), Bacterial stress responses. ASM Press, Washington, DC.
14. **Gilmour, R., P. Messner, A. A. Guffanti, R. Kent, A. Scheberl, N. Kendrick, and T. A. Krulwich.** 2000. Two-dimensional gel electrophoresis analyses of pH-dependent protein expression in facultatively alkaliphilic *Bacillus pseudofirmus* OF4 lead to characterization of an S-layer protein with a role in alkaliphily. J. Bacteriol. **182:**5969–5981.
15. **Goldberg, E. B., T. Arbel, J. Chen, R. Karpel, G. A. Mackie, S. Schuldiner, and E. Padan.** 1987. Characterization of a Na^+/H^+ antiporter gene of *Escherichia coli*. Proc. Natl. Acad. Sci. USA **84:**2615–2619.
16. **Grunwald, C.** 1974. Sterol molecular modifications influencing membrane permeability. Plant Physiol. **54:**624–628.
17. **Haines, T. H.** 2001. Do sterols reduce proton and sodium leaks through lipid bilayers? Prog. Lipid Res. **40:**299–324.
18. **Hauss, T., S. Dante, N. A. Dencher, and T. H. Haines.** 2002. Squalane is in the midplane of the lipid bilayer: implications for its function as a proton permeability barrier. Biochim. Biophys. Acta **1556:**149–154.
19. **Horbach, S., B. Neuss, and H. Sahm.** 1991. Effect of azasqualene on hopanoid biosynthesis and ethanol tolerance of *Zymomonas mobilis*. FEMS Microbiol. Lett. **79:**347–350.
20. **Hossack, J. A., and A. H. Rose.** 1976. Fragility of plasma membranes in *Saccharomyces cerevisiae* enriched with different sterols. J. Bacteriol. **127:**67–75.
21. **Jahnke, L. L., H. Stan-Lotter, K. Kato, and L. I. Hochstein.** 1992. Presence of methyl sterol and bacteriohopanepolyol in an outer-membrane preparation from *Methylococcus capsulatus* Bath. J. Gen. Microbiol. **138:**1759–1766.
22. **Jiao, Y., A. Kappler, L. R. Croal, and D. K. Newman.** 2005. Isolation and characterization of a genetically tractable photoautotrophic Fe(II)-oxidizing bacterium, *Rhodopseudomonas palustris* strain TIE-1. Appl. Environ. Microbiol. **71:**4487–4496.
23. **Jiao, Y., and D. K. Newman.** 2007. The *pio* operon is essential for phototrophic Fe(II) oxidation in *Rhodopseudomonas palustris* TIE-1. J. Bacteriol. **189:**1765–1773.
24. **Jurgens, U. J., P. Simonin, and M. Rohmer.** 1992. Localization and distribution of hopanoids in membrane systems of the cyanobacterium *Synechocystis* PCC 6714. FEMS Microbiol. Lett. **71:**285–288.
25. **Keen, N. T., S. Tamaki, D. Kobayashi, and D. Trollinger.** 1988. Improved broad-host-range plasmids for DNA cloning in gram-negative bacteria. Gene **70:**191–197.
26. **Kleemann, G., R. Kellner, and K. Poralla.** 1994. Purification and properties of the squalene-hopene cyclase from *Rhodopseudomonas palustris*, a purple non-sulfur bacterium producing hopanoids and tetrahymanol. Biochim. Biophys. Acta **1210:**317–320.
27. **Kovach, M. E., P. H. Elzer, D. S. Hill, G. T. Robertson, M. A. Farris, R. M. Roop II, and K. M. Peterson.** 1995. Four new derivatives of the broad-host-range cloning vector pBBR1MCS, carrying different antibiotic-resistance cassettes. Gene **166:**175–176.
28. **Lewinson, O., E. Padan, and E. Bibi.** 2004. Alkalitolerance: a biological function for a multidrug transporter in pH homeostasis. Proc. Natl. Acad. Sci. USA **101:**14073–14078.
29. **Maurer, L. M., E. Yohannes, S. S. Bondurant, M. Radmacher, and J. L. Slonczewski.** 2005. pH regulates genes for flagellar motility, catabolism, and oxidative stress in *Escherichia coli* K-12. J. Bacteriol. **187:**304–319.
30. **Nalin, R., S. R. Putra, A. M. Domenach, M. Rohmer, F. Gourbiere, and A. M. Berry.** 2000. High hopanoid/total lipids ratio in *Frankia* mycelia is not related to the nitrogen status. Microbiology **146:**3013–3019.
31. **Neunlist, S., P. Bisseret, and M. Rohmer.** 1988. The hopanoids of the purple non-sulfur bacteria *Rhodopseudomonas palustris* and *Rhodopseudomonas acidophila* and the absolute configuration of bacteriohopanetetrol. Eur. J. Biochem. **171:**245–252.
32. **Oda, Y., F. W. Larimer, P. S. Chain, S. Malfatti, M. V. Shin, L. M. Vergez, L. Hauser, M. L. Land, S. Braatsch, J. T. Beatty, D. A. Pelletier, A. L. Schaefer, and C. S. Harwood.** 2008. Multiple genome sequences reveal adaptations of a phototrophic bacterium to sediment microenvironments. Proc. Natl. Acad. Sci. USA **105:**18543–18548.
33. **Oda, Y., W. Wanders, L. A. Huisman, W. G. Meijer, J. C. Gottschal, and L. J. Forney.** 2002. Genotypic and phenotypic diversity within species of purple nonsulfur bacteria isolated from aquatic sediments. Appl. Environ. Microbiol. **68:**3467–3477.
34. **Ourisson, G., and P. Albrecht.** 1992. Hopanoids. 1. Geohopanoids—the most abundant natural products on Earth. Acc. Chem. Res. **25:**398–402.
35. **Ourisson, G., P. Albrecht, and M. Rohmer.** 1979. Hopanoids—palaeochemistry and biochemistry of a group of natural products. Pure Appl. Chem. **51:**709–729.
36. **Ourisson, G., M. Rohmer, and K. Poralla.** 1987. Prokaryotic hopanoids and other polyterpenoid sterol surrogates. Annu. Rev. Microbiol. **41:**301–333.
37. **Padan, E., E. Bibi, M. Ito, and T. A. Krulwich.** 2005. Alkaline pH homeostasis in bacteria: new insights. Biochim. Biophys. Acta **1717:**67–88.
38. **Padan, E., N. Maisler, D. Taglicht, R. Karpel, and S. Schuldiner.** 1989. Deletion of *ant* in *Escherichia coli* reveals its function in adaptation to high salinity and an alternative Na^+/H^+ antiporter system(s). J. Biol. Chem. **264:**20297–20302.
39. **Parales, R. E., and C. S. Harwood.** 1993. Regulation of the *pcaIJ* genes for aromatic acid degradation in *Pseudomonas putida*. J. Bacteriol. **175:**5829–5838.
40. **Parks, L. W., and W. M. Casey.** 1995. Physiological implications of sterol biosynthesis in yeast. Annu. Rev. Microbiol. **49:**95–116.
41. **Peng, L., Y. Kawagoe, P. Hogan, and D. Delmer.** 2002. Sitosterol-beta-glucoside as primer for cellulose synthesis in plants. Science **295:**147–150.
42. **Perzl, M., I. G. Reipen, S. Schmitz, K. Poralla, H. Sahm, G. A. Sprenger, and E. L. Kannenberg.** 1998. Cloning of conserved genes from *Zymomonas mobilis* and *Bradyrhizobium japonicum* that function in the biosynthesis of hopanoid lipids. Biochim. Biophys. Acta **1393:**108–118.
43. **Poralla, K., T. Hartner, and E. Kannenberg.** 1984. Effect of temperature and pH on the hopanoid content of *Bacillus acidocaldarius*. FEMS Microbiol. Lett. **23:**253–256.
44. **Poralla, K., G. Muth, and T. Hartner.** 2000. Hopanoids are formed during transition from substrate to aerial hyphae in *Streptomyces coelicolor* A3(2). FEMS Microbiol. Lett. **189:**93–95.
45. **Price-Whelan, A., L. E. Dietrich, and D. K. Newman.** 2007. Pyocyanin alters redox homeostasis and carbon flux through central metabolic pathways in *Pseudomonas aeruginosa* PA14. J. Bacteriol. **189:**6372–6381.
46. **Quandt, J., and M. F. Hynes.** 1993. Versatile suicide vectors which allow direct selection for gene replacement in gram-negative bacteria. Gene **127:**15–21.
47. **Rajakumari, S., K. Grillitsch, and G. Daum.** 2008. Synthesis and turnover of non-polar lipids in yeast. Prog. Lipid Res. **47:**157–171.
48. **Rashby, S. E., A. L. Sessions, R. E. Summons, and D. K. Newman.** 2007. Biosynthesis of 2-methylbacteriohopanepolyols by an anoxygenic phototroph. Proc. Natl. Acad. Sci. USA **104:**15099–15104.
49. **Rohmer, M., P. Bouviernave, and G. Ourisson.** 1984. Distribution of hopanoid triterpenes in prokaryotes. J. Gen. Microbiol. **130:**1137–1150.
50. **Rozen, S., and H. Skaletsky.** 2000. Primer3 on the WWW for general users and for biologist programmers. Methods Mol. Biol. **132:**365–386.
51. **Ruiz, N., B. Falcone, D. Kahne, and T. J. Silhavy.** 2005. Chemical conditionality: a genetic strategy to probe organelle assembly. Cell **121:**307–317.
52. **Schuldiner, S., V. Agmon, J. Brandsma, A. Cohen, E. Friedman, and E. Padan.** 1986. Induction of SOS functions by alkaline intracellular pH in *Escherichia coli*. J. Bacteriol. **168:**936–939.

53. **Simon, R., U. Priefer, and A. Puhler.** 1983. A broad host range mobilization system for *in vivo* genetic engineering: transposon mutagenesis in gram-negative bacteria. Biotechnology **1:**784–791.
54. **Simonin, P., U. J. Jurgens, and M. Rohmer.** 1996. Bacterial triterpenoids of the hopane series from the prochlorophyte *Prochlorothrix hollandica* and their intracellular localization. Eur. J. Biochem. **241:**865–871.
55. **Summons, R. E., and L. L. Jahnke.** 1992. Hopenes and hopanes methylated in ring-A: correlation of the hopanoids of extant methylotrophic bacteria with their fossil analogues, p. 189–200. *In* J. M. Moldowan, P. Albrecht, and R. P. Philip (ed.), Biomarkers in sediments and petroleum. Prentice Hall, Englewood Cliffs, NJ.
56. **Summons, R. E., L. L. Jahnke, J. M. Hope, and G. A. Logan.** 1999. 2-Methylhopanoids as biomarkers for cyanobacterial oxygenic photosynthesis. Nature **400:**554–557.
57. **Swan, T. M., and K. Watson.** 1998. Stress tolerance in a yeast sterol auxotroph: role of ergosterol, heat shock proteins and trehalose. FEMS Microbiol. Lett. **169:**191–197.
58. **Taglicht, D., E. Padan, A. B. Oppenheim, and S. Schuldiner.** 1987. An alkaline shift induces the heat shock response in *Escherichia coli*. J. Bacteriol. **169:**885–887.
59. **Talbot, H. M., R. E. Summons, L. L. Jahnke, C. S. Cockell, M. Rohmer, and P. Farrimond.** 2008. Cyanobacterial bacteriohopanepolyol signatures from cultures and natural environmental settings. Org. Geochem. **39:**232–263.
60. **Ten Haven, H. L., M. Rohmer, J. Rullkotter, and P. Bisseret.** 1989. Tetrahymanol, the most likely precursor of gammacerane, occurs ubiquitously in marine sediments. Geochim. Cosmochim. Acta **53:**3073–3079.
61. **Thomas, D. S., J. A. Hossack, and A. H. Rose.** 1978. Plasma-membrane lipid composition and ethanol tolerance in *Saccharomyces cerevisiae*. Arch. Microbiol. **117:**239–245.
62. **Wilks, J. C., and J. L. Slonczewski.** 2007. pH of the cytoplasm and periplasm of *Escherichia coli*: rapid measurement by green fluorescent protein fluorimetry. J. Bacteriol. **189:**5601–5607.
63. **Zilberstein, D., V. Agmon, S. Schuldiner, and E. Padan.** 1984. *Escherichia coli* intracellular pH, membrane potential, and cell growth. J. Bacteriol. **158:**246–252.
64. **Zundel, M., and M. Rohmer.** 1985. Prokaryotic triterpenoids 1. 3 β-Methylhopanoids from *Acetobacter* species and *Methylococcus capsulatus*. Eur. J. Biochem. **150:**23–27.